
Article:
Tao, R., Liu, W., Chu, X. orcid.org/0000-0003-1863-6149 et al. (1 more author) (2019) An energy saving small cell sleeping mechanism with cell range expansion in heterogeneous networks. IEEE Transactions on Wireless Communications, 18 (5). pp. 2451-2463. ISSN 1536-1276

https://doi.org/10.1109/TWC.2019.2895028

An Energy Saving Small Cell Sleeping Mechanism with Cell Range Expansion in Heterogeneous Networks

Ran Tao, Wuling Liu, Xiaoli Chu, Jie Zhang

***Abstract*—In recent years, the explosion of wireless data traffic has resulted in a trend of a large scale dense deployment of small cells, with which the rising cost of energy has attracted a lot of research interest. In this paper, we present a novel sleeping mechanism for small cells to decrease the energy consumption of heterogeneous networks (HetNets). Specifically, in the cell-edge area of a macrocell, small cells will be put into sleep where possible and their service areas will be covered by range-expanded small cells nearby and the macrocell; in areas close to the macrocell, User equipments (UEs) associated with a sleeping small cell will be handed over to the macrocell. Furthermore, we use enhanced inter-cell interference coordination (eICIC) techniques to support range expanded small cells to avoid QoS degradation. Using a stochastic geometry based network model, we provide the numerical analysis of the proposed approach, and the results indicate that the proposed sleeping mechanism can significantly reduce the power consumption of the network compared with the existing sleeping methods while guaranteeing the QoS requirement.**

***Index Terms*—Stochastic geometry, small cell, sleeping mode, energy efficiency, HetNets.**

I. Introduction

The amount of data usage has been doubled each year during the last few years. One way to meet the explosive data demand is to deploy small cells in a large scale [1]. However, increasing the density of small cells will cause economic and environmental problems due to the increasing power consumption and CO_2 emissions. Current research shows that the amount of CO_2 emissions due to the information and communication technology (ICT) industry has already reached 2% [2]–[4] and it could reach to 3.6% by 2020 and up to 14% by 2040 [5]. In addition, the communication technology (CT) has consumed around 10% global electricity in 2016, and it is forecasted that the share will rise up to 21% by 2030 [6]. Therefore, energy savings become increasingly crucial for cellular networks. Recent researches take energy saving into consideration by adapting base station (BS) density, ie., switching on/off BSs to the dynamic traffic demand [7].

A. Related Work

The authors in [8], [9] presented macrocell range expansion mechanisms based on adaptive cell zooming with varying traffic loads. In [10], the authors proposed a network-impact switching-on/off algorithm that can be operated in a distributed manner with low computational complexity. In [11], the authors proposed a cell sleeping algorithm to switch off low load cells and compensating for the coverage loss by expanding the neighbouring cells through antenna beam tilting. In [12], the authors proposed several switch-off patterns in homogeneous networks with different service arrival rates, where the coordinated multiple point (CoMP) transmission technology was used to extend cell coverage. In [13], the authors proposed an energy saving mechanism for LTE networks to decide whether or not to switch off an eNodeB (eNB) based on the average distance of its associated UEs. In [14], the authors made a conclusion that the cell sleeping mode operation is effective in energy saving when the traffic is light and cell size is small. In [15], an energy saving mechanism was used to reduce the number of active BSs while guaranteeing the coverage probability.

Recent efforts related to cell sleeping modes have been made in small cell networks. In [16], the authors provided a fixed time sleeping scheme to save the energy of femtocells. In [17], [18], the authors proposed a sleep mode mechanism in dense small cell networks, which switched off idle small cells or cells with few UEs.

All the existing works mentioned above focused on homogeneous networks. More recently, BS sleeping mode has also been studied for HetNets energy saving. In [19], an optimal sleep/wake-up mechanism was provided to maximize the energy saving of the HetNets. In [20], the authors provided a repulsive cell activation scheme considering the minimum separation distance between the small cells to achieve improved energy efficiency. In [21], the authors derived the energy efficiency in homogeneous and heterogeneous networks with various sleeping strategies. In [22], a numerical analysis of a random sleeping strategy and a simulation based sleeping mechanism were presented. In [23], the authors analysed the optimal BS density that minimizes the network energy consumption for both homogeneous and heterogeneous networks. In [24], the authors proposed a sleeping control scheme by switching off small cells with low traffic load and offloading the traffic to their nearest macrocells. In [25], the authors only demonstrated that switching off small cells closer to macrocells achieves higher energy efficiency, but no small cell sleeping mechanism was proposed. In [26], a small cell activation mechanism for HetNets was proposed. The authors maximized the network energy saving by considering the

This work was funded by the EUs H2020 research and innovation programme under the grant agreement No 645705. (Corresponding author: Ran Tao.)

Ran Tao, Wuling Liu, Xiaoli Chu, Jie Zhang are with the Department of Electronic and Electrical Engineering, The University of Sheffield, Sheffield S10 2TN, UK, e-mail: (elp12rt@sheffield.ac.uk; wuling.liu@sheffield.ac.uk; x.chu@sheffield.ac.uk; jie.zhang@sheffield.ac.uk).

traffic load transferred from macrocells to the active small cells. In [27]–[29], the authors studied the energy saving of HetNets by turning off small cells close to macrocells.

In order to avoid QoS degradation of the UEs from cell edge of range-expanded small cells, we use the eICIC technique to ensure their QoS requirements. Research in [30], [31] shows that eICIC technique is an effective way to improve the QoS performance of cell edge UEs.

B. Small Cell Sleeping Strategy

- Proposed Sleeping Strategy: In this paper, we propose an energy-saving small cell sleeping mechanism in a HetNet. Just as Fig. 1 shows, the small cells whose distance to the macrocell smaller than z are all pushed into sleeping mode. Furthermore, we control the density of the remaining small cells by using cell range expansion (CRE) technique. It is noted that as the UEs inside the dashed circle are close to the macrocell, we make the assumption that all the UEs from the sleeping cells within the dashed circle can only be offloaded to the macrocell. We also use the eICIC technique to effectively improve the QoS of UEs in the edge of small cells. The macrocell can mute its downlink transmissions in specific subframes called almost blank subframes (ABSs). In this paper, we assume that ABSs are allocated only to the UEs in the small cell range expansion area to avoid the interference from the macrocell. The UEs located close to the small cells and in the coverage of the macrocell are scheduled with normal subframes.
  In existing works [27], [28], the authors only switched off small cells close to the macrocell and handed over the associated UEs to the macrocell. However, we notice that the network power saving of this kind of approach is not significant, because many small cells in the area far from the macrocell are still active.
- Conventional Sleeping Strategy: We select the repulsive sleeping scheme in [27] as the conventional method in our paper. We turn off the small cells inside a circle around the macrocell and hand over the associated UEs to the macrocell.
- Random Sleeping: Each small cell has an equal probability to be put into sleep mode.

C. Contributions

- We propose to combine adaptive small cell expansion (cell zooming) and small cell sleeping mechanism. More specifically, we propose to use range expanded small cells to cover the traffic from nearby sleeping small cells in the edge area of the macrocell in order to save more power. This is different from the existing small cell sleeping mechanism [27], where all the traffic of a sleeping small cell would be handed over to the macrocell to reduce the network power consumption. Furthermore, eICIC technique is applied in conjunction with cell range expansion to guarantee the QoS of UEs in the edge area of small cells.
- For the proposed small cell sleeping mechanism, we provide a detailed analysis of the resulting inter-cell interference. We consider the fact that under the repulsive sleeping mechanism, almost all the small cells close to the macrocell are turned off and excluded from the set of the interferers. This analysis is more accurate than that in [20], where the small cell density is assumed to be uniformly decreased across the whole area in the interference analysis.
- We derive the expressions for association probability and coverage probability under the proposed small cell sleeping mechanism in a two-tier HetNet.
- We jointly optimize the cell range bias factor (B_2), small cell density, and switching off radius (z) to minimize the network power consumption for a given UE density. A genetic algorithm (GA) is proposed to solve the joint optimization problem at a reduced computational complexity.
- For a given traffic profile, we show that our proposed small cell sleeping mechanism achieves a much lower network power consumption compared with random and conventional ones, especially in a high UE density scenario.

The rest of this paper is organized as follows. Section II describes the system model. In Section III, we derive the coverage probability of UEs in different sets. The comparison between the numerically based coverage probability and corresponding simulation results is provided in Section IV. Then, the problem analysis is given in in Section V followed by conclusions in Section VI.

II. System Model

A. Downlink System Model

In our system model, we consider a two-tier HetNet with a macrocell (tier 1) and small cells (tier 2). Since the macrocells' locations should be carefully designed to maintain their coverage, in our model, the macrocells are considered to be regularly deployed as hexagonal cells. On the contrary, small cells are densely deployed to boost the network capacity, hence the small cells are assumed to form a homogeneous Poison Point Process (HPPP) with intensity λ_2 as shown in Fig. 1. We assume that the active UEs are uniformly distributed in the network coverage area and the UE density is expressed as $\lambda_u(t)$ at time t.

Both macrocells and small cells are assumed to share the same frequency band. Each BS has a limited bandwidth denoted as W here. We also suppose that all BSs in the same tier transmit with an equal fixed power P_k, where $k = 1$ for the first tier and $k = 2$ for the second tier. The downlink desired and interference signals from a BS of tier-k are assumed to experience pathloss with distance exponent α_k. The received power of a UE from a BS of the k^{th} tier at a distance x can be expressed as $P_k h_x x^{-\alpha_k}$, where h_x is the random channel power gain which is assumed to be exponentially distributed with mean $\mu = 1$.

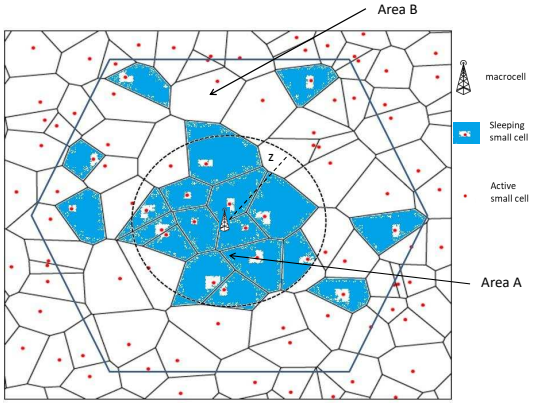

Fig. 1. Illustration of our system model

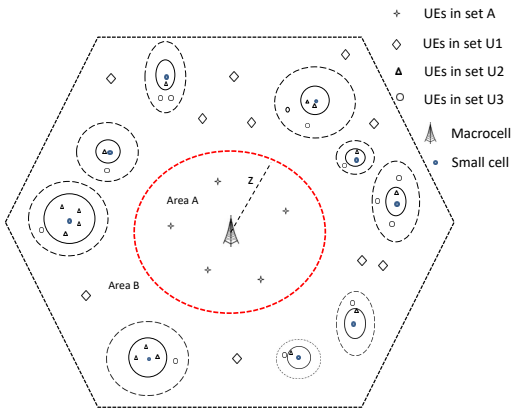

Fig. 2. Illustration of our UE association model

Let d_k denote the distance of a typical UE from the nearest BS of the k^{th} tier. It is assumed that each UE will connect to the BS based on the following rule:

$$j = \arg \max_{k \in \{1,2\}} \{P_k B_k d_k^{-\alpha_k}\}, \tag{1}$$

where B_k is the cell association bias factor for the k^{th} tier. In this paper, we only consider the association bias for tier 2 (small cell tier), which is denoted as B_2 here. Fig.1 illustrates our system model. We name the area inside the dashed circle with radius z as area A and the area outside of the dashed circle as area B. We assume that all small cells within area A are switched off and the associated UEs will be handed over to the macrocell. In area B, small cells are partially turned off.

In the given setup, a user u can be in the area A connected to the macrocell, named set A here, and the following three disjoint sets, where j is expressed in (1):

$$u \in \begin{cases} U_1 \ if \ j = 1, \ P_1 R_1^{-\alpha_1} \geq P_2 R_2^{-\alpha_2} B_2, \\ U_2 \ if \ j = 2, \ P_2 R_2^{-\alpha_2} \geq P_1 R_1^{-\alpha_1}, \\ U_3 \ if \ j = 2, \ P_2 R_2^{-\alpha_2} \leq P_1 R_1^{-\alpha_1} < P_2 R_2^{-\alpha_2} B_2, \end{cases} \tag{2}$$

where set U_1 is the set of UEs in the area outside of the dashed circle connected to the macrocell, set U_2 is the set of unbiased small cell UEs in the area outside of the dashed line circle. Set U_3 is the set of biased UEs in the area outside of the dashed circle. Fig. 2 is displayed to illustrate our UE association model.

For a typical UE_u in set A or set U_1, the received SINR is given as :

$$\gamma_u = \frac{P_1 h_{m,u} d_{m,u}^{-\alpha_1}}{\sum_{i \in \mathcal{C}_2} h_{i,u} d_{i,u}^{-\alpha_2} P_2 + \sigma^2}, \tag{3}$$

where P_1 is the transmit power of a macrocell, $h_{m,u}$ is the exponential fading power gain of the link from the macrocell to UE_u, and $h_{i,u}$ are the exponential fading power gain of interfering link from small cell i to UE_u, $d_{m,u}$ is the distance between the macrocell and UE_u, and $d_{i,u}$ is the distances from interfering small cell i to the UE_u, and $\mathcal{C}_2$ is the set of all the small cells. σ^2 is the noise power.

For a typical UE_u in set U_2, the received SINR can be expressed as follows:

$$\gamma_u = \frac{P_2 h_{l,u} d_{l,u}^{-\alpha_2}}{\sum_{i \in \mathcal{C}_2 \setminus l} h_{i,u} d_{i,u}^{-\alpha_2} P_2 + I_m + \sigma^2}, \tag{4}$$

where P_2 is the transmit power of a macrocell, $h_{l,u}$ is the exponential fading power gain of the link from the serving small cell l to the UE_u, and $h_{i,u}$ are the exponential fading power gain of interfering links from other small cells to the UE_u. $d_{l,u}$ is the distance between the serving small cell l to the UE_u, and $d_{i,u}$ is the distance from interfering small cell i to the UE_u. $\mathcal{C}_2$ is the set of interfering small cells. I_m is the interference from the macrocell. σ^2 is the noise power.

For a typical UE_u in set U_3, the received SINR can be expressed as follows:

$$\gamma_u = \frac{P_2 h_{l,u} d_{l,u}^{-\alpha_2}}{\sum_{i \in \mathcal{C}_2 \setminus l} h_{i,u} d_{i,u}^{-\alpha_2} P_2 + \sigma^2}. \tag{5}$$

Assuming each macrocell allocates bandwidth equally to its active UEs, the achievable data rate of UE_u can be written as:

$$r_u = \frac{W}{N} \log_2(1 + \gamma_u), \tag{6}$$

where N is the number of active UEs associated to the serving BS, W is the bandwidth allocated to the serving BS, γ_u is the SINR for UE_u which can be found in (3), (4) and (5). The coverage probability here is defined as the probability that the data rate of UE_u is above the threshold U, which can be expressed as $\mathbb{P}\{r_u > U\}$.

The service coverage constraint of UE_u can be expressed as:

$$\mathbb{P}\left(\frac{W}{N} \log_2(1 + \gamma_u) > U\right) > \eta, \tag{7}$$

where η is the threshold of the coverage probability.

B. Power Consumption Model

In this paper, the power consumption model can be expressed as [26]:

$$P_C = \begin{cases} N_{AT}(P_{0(i)} + \Delta_{p(i)}P_{t(i)}), & 0 < P_{t(i)} \le P_{M(i)}, \\ N_{AT}P_{s(i)}, & P_{t(i)} = 0, \end{cases} \tag{8}$$

where i=s or m, representing small cell or macrocell, N_{AT} is the number of antennas used at the BSs, $P_{0(i)}$ is the static power consumption, $\Delta_{p(i)}$ is the slope of the power model, $P_{s(i)}$ is the power consumption for the BS in sleep model, in this paper we assume $P_{s(s)} = 0$ without loss of generality, $P_{t(i)}$ is the RMS transmit power which can be expressed as: $P_{t(i)} = \rho * P_{M(i)}$, where ρ is the load of the BS and P_M is the maximum RMS transmit power of the BS. The value of the parameters above are all listed in Table I [26].

III. Coverage Probability Analysis for Proposed Strategy Sleeping Policy

In this section, we will derive the coverage probability of UEs in set A, U_1, U_2, and U_3, which will be verified by our simulation in section IV. The distance between a typical UE in area B with the macrocell and its nearest small cell is denoted as R_1 and R_2 respectively. In addition, without loss of generality, we suppose $\alpha_1 = \alpha_2 = 4$. The assumption of the same pathloss exponent for macrocells and small cells has been used in many existing works, e.g., [21]–[23], [32], [33]. In [21], [22], the authors make the assumption that the pathloss exponent equal to 4. Furthermore, for simplicity, we average the interference from the macrocell to the UEs in set U_2, which can be written as: $\mathrm{E}[I_m] = \int_z^R P_1 r^{-\alpha_1} \frac{2r}{R^2-z^2}\,\mathrm{d}r$, where R is the radius of the macrocell. We also assume that all the small cells inside radius z are all switched off, just as shown in Fig. 1.

1) UEs in set A: In this part, the coverage probability of UEs in set A will be derived.

The Probability density function (PDF) $f_R(r)$ of the distance R between a random UE in area A and the associated macrocell can be expressed as :

$$f_R(r) = \frac{2r}{z^2}. \tag{9}$$

Theorem 1. *The coverage probability for UEs in area A can be given as:*

$$G_A = \int_0^z e^{-\mu T r^{\alpha_1}\sigma^2}\mathcal{L}_{I_s}(\mu T r^{\alpha_1})\frac{2r}{z^2}\,\mathrm{d}r, \tag{10}$$

where $T = \frac{2^{\frac{UN_A}{W_A}}-1}{P_1}$, *$N_A$ is the number of UEs in set A and can be expressed as: $N_A = \lambda_u \pi z^2$, W_A is bandwidth allocated to UEs in set A, and $\mathcal{L}_{I_s}(\mu T r^{\alpha_1})$ can be written as:*

$$\begin{aligned}\mathcal{L}_{I_s}(\mu T r^{\alpha_1}) = &\exp\left(-\pi r^2\lambda_2(T\cdot P_2)^{2/\alpha}(\pi/2)\right) \\ &\times \exp\left(2\lambda_2\int_{r-z}^{r+z}\frac{\arccos(\frac{r^2+\rho^2-z^2}{2r\rho})}{1+\frac{\rho^{\alpha_2}}{P_2 s}}\rho\,\mathrm{d}\rho\right) \\ &\times \exp\left(2\lambda_2\int_0^{r-z}\frac{\pi}{1+\frac{\rho^{\alpha_2}}{P_2 s}}\rho\,\mathrm{d}\rho\right).\end{aligned} \tag{11}$$

Proof: See Appendix A. ∎

2) UEs in set U_1: In this section, we focus on computing the coverage probability for UEs in set U_1. Just as shown in Fig. 2, set U_1 is the set of UEs connected to the macrocell in area B. The set is expressed in (2).

The probability that a UE in set U_1 can be expressed as:

$$\begin{aligned} q_{U_1} &= \mathbb{P}(P_1 R_1^{-\alpha_1} \ge P_2 R_2^{-\alpha_2} B_2) \\ &= \int_z^R \mathbb{P}(R_2 \ge ((\frac{P_1}{P_2 B_2})^{-\frac{1}{\alpha_2}} R_1^{\frac{\alpha_1}{\alpha_2}}) f_{R_1}(r)\,\mathrm{d}r \\ &= \int_z^R e^{-\lambda_2(\frac{P_1}{P_2 B_2})^{-\frac{2}{\alpha_2}} r^{\frac{2\alpha_1}{\alpha_2}}} \frac{2r}{R^2-z^2}\,\mathrm{d}r. \end{aligned} \tag{12}$$

The number of users in set U_1 can be expressed as $N_{U_1} = q_{U_1}\pi(R^2-z^2)$.

Theorem 2. *The PDF $f_{X_1}(x)$ of the distance X_1 between a random UE in set U_1 with its associated macrocell is :*

$$\begin{aligned} f_{X_1}(x) &= \frac{dF_{X1}}{dx} \\ &= \begin{cases} 0, & x \le z. \\ \frac{1}{q_{U_1}} e^{(-\lambda_2\pi(\frac{P_1}{P_2 B_2})^{-\frac{2}{\alpha_2}} x^{\frac{2\alpha_1}{\alpha_2}})} \frac{2x}{R^2-z^2}, & R \ge x > z. \\ 0, & x > R. \end{cases} \end{aligned} \tag{13}$$

Proof: The event of $X_1 > x$ is the event of $R_1 > x$ conditioned on the UE's association to the first tier. The probability of $X_1 > x$ can be expressed as

$$\mathbb{P}[X_1 > x] = \frac{\mathbb{P}[R_1 > x, n = 1]}{\mathbb{P}[n = 1]}, \tag{14}$$

where $\mathbb{P}[n = 1]$ is the probability of a UE in set U_1, which is given in (12). The joint probability of $R_1 > r$ and n=1 is:

$$\begin{aligned} &\mathbb{P}[R_1 > x, n = 1] \\ &= \mathbb{P}[R_1 > x, P_1 R_1^{-\alpha_1} \ge P_2 R_2^{-\alpha_2} B_2)] \\ &= \int \mathbb{P}\left[r > x, (R_2 \ge ((\frac{P_1}{P_2 B_2})^{-\frac{1}{\alpha_2}} r^{\frac{\alpha_1}{\alpha_2}})\right] f_{R_1}(r)\,\mathrm{d}r \\ &= \int_z^R \mathbb{P}\left[r > x, (R_2 \ge ((\frac{P_1}{P_2 B_2})^{-\frac{1}{\alpha_2}} r^{\frac{\alpha_1}{\alpha_2}})\right] \frac{2r}{R^2-z^2}\,\mathrm{d}r. \end{aligned} \tag{15}$$

Solving (15), $\mathbb{P}[R_1 > x, n = 1]$ can be derived as:

$$\begin{aligned} &\mathbb{P}[R_1 > x, n = 1] \\ &= \begin{cases} \int_z^R e^{(-\lambda_2\pi(\frac{P_1}{P_2 B_2})^{-\frac{2}{\alpha_2}} r^{\frac{2\alpha_1}{\alpha_2}})} \frac{2r}{R^2-z^2}\,\mathrm{d}r, x \le z, \\ \int_x^R e^{(-\lambda_2\pi(\frac{P_1}{P_2 B_2})^{-\frac{2}{\alpha_2}} r^{\frac{2\alpha_1}{\alpha_2}})} \frac{2r}{R^2-z^2}\,\mathrm{d}r, R \ge x > z, \\ 0, \quad x > R. \end{cases} \end{aligned} \tag{16}$$

∎

The Cumulative density function (CDF) of X_1 can be expressed as:

$$\begin{aligned} F_{X_1}(x) &= 1 - \mathbb{P}[X_1 > x] \\ &= 1 - \frac{1}{q_{U_1}}\mathbb{P}[R_1 > x, n = 1]. \end{aligned} \tag{17}$$

The PDF of X_1 is :

$$f_{X_1}(x) = \frac{dF_{X_1}}{dx} = \begin{cases} 0, & x \le z, \\ \frac{1}{q_{U_1}} e^{(-\lambda_2 \pi (\frac{P_1}{P_2 B_2})^{-\frac{2}{\alpha_2}} x^{\frac{2\alpha_1}{\alpha_2}})} \frac{2x}{R^2 - z^2}, & R \ge x > z, \\ 0, & x > R. \end{cases} \tag{18}$$

Corollary 1. *The coverage probability of UEs in set U_1 can be expressed as:*

$$G_{U_1} = \int_z^R e^{-\lambda_2 \pi (\frac{P_1}{P_2 B_2})^{-\frac{2}{\alpha_2}} x^{\frac{2\alpha_1}{\alpha_2}}} e^{-\mu T x^{\alpha_1} \sigma^2} \times \mathcal{L}_{I_s}(\mu T x^{\alpha_1}) \frac{2x}{q_{U_1}(R^2 - z^2)} \, \mathrm{d}x, \tag{19}$$

where $T = \frac{2^{\frac{U * N_{U_1}}{W_{U_1}}} - 1}{P_1}$, W_{U_1} is the bandwidth allocated to UEs in set U_1, N_{U_1} is the average number of UEs in set U_1 and can be expressed as: $N_{U_1} = q_{U_1} \frac{\lambda_u}{\lambda_2}$, and

$$\mathcal{L}_{I_s}(\mu T x^{\alpha_1}) = \exp\left(\int_g^{x+z} \frac{2\pi l(\rho)}{1 + \frac{\rho^{\alpha_2}}{P_2 \cdot s}} \rho \mathrm{d}\rho \right) \times \exp\left(-\lambda_2 \pi x^2 (T P_2)^{2/\alpha} \operatorname{arccot}(m T^{-2/\alpha}) \right), \tag{20}$$

where $l(\rho) = \frac{\lambda_2}{\pi} \arccos(\frac{x^2 + \rho^2 - z^2}{2x\rho})$, $m = (\frac{P_1}{P_2 B_2})^{-2/\alpha_2}$, $g = \max[x - z, (\frac{P_1}{P_2 B_2})^{-1/\alpha_2} \cdot x]$.

Proof: See Appendix B. ∎

3) UEs in Set U_2: In this section, we will give an analysis of the coverage probability of UEs in set U_2. Just as shown in Fig. 2, set U_2 is the set of UEs close to small cells in area B. The set is expressed in (2).

The probability that a UE in set U_2 is:

$$\begin{aligned} q_{U_2} =& \mathbb{P}(P_2 R_2^{-\alpha_2} \ge P_1 R_1^{-\alpha_1}) \\ =& \int_z^R \mathbb{P}(R_2 \le (\frac{P_1}{P_2})^{-\frac{1}{\alpha_2}} R_1^{\frac{\alpha_1}{\alpha_2}}) f_{R_1}(r) \, \mathrm{d}r \\ =& \int_z^R (1 - e^{-\pi \lambda_2 ((\frac{P_1}{P_2})^{-\frac{2}{\alpha_2}} r^{\frac{2\alpha_1}{\alpha_2}})}) \frac{2r}{R^2 - z^2} \, \mathrm{d}r. \end{aligned} \tag{21}$$

Theorem 3. *The PDF $f_{X_2}(x)$ of the distance X_2 between a random UE in set U_2 with its associated small cell is:*

$$f_{X_2}(x) = \frac{dF_{X_2}}{dx} = \begin{cases} \frac{1}{q_{U_2}} (2\pi \lambda_2 x e^{-\lambda_2 \pi x^2}), & x \le x_1, \\ \frac{R^2 - (\frac{P_2}{P_1})^{-\frac{2}{\alpha_1}} x^{\frac{2\alpha_2}{\alpha_1}}}{R^2 - z^2} \frac{2\pi \lambda_2}{q_{U_2}} x e^{-\lambda_2 \pi x^2}, & x_2 \ge x > x_1, \\ 0, & x > x_2, \end{cases} \tag{22}$$

where $x_1 = \frac{z}{(P_2/P_1)^{-0.25}}$ and $x_2 = \frac{R}{(P_2/P_1)^{-0.25}}$,

Proof: The event of $X_2 > x$ is the event of $R_2 > x$ conditioned on the UE's association to the second tier. The probability of $X_2 > x$ can be expressed as

$$\mathbb{P}[X_2 > x] = \frac{\mathbb{P}[R_2 > x, n = 2]}{\mathbb{P}[n = 2]}, \tag{23}$$

where $\mathbb{P}[n = 2]$ is the probability that a UE in set U_2, which is expressed in (21). The joint probability of $R_2 > x$ and n=2 is:

$$\begin{aligned} &\mathbb{P}[R_2 > x, n = 2] \\ &= \mathbb{P}[R_2 > x, P_2 R_2^{-\alpha_2} \ge P_1 R_1^{-\alpha_1})] \\ &= \int \mathbb{P}[r > x, (R_1 \ge ((\frac{P_2}{P_1})^{-\frac{1}{\alpha_1}} r^{\frac{\alpha_2}{\alpha_1}})] f_{R_2}(r) \, \mathrm{d}r \\ &= \int \mathbb{P}[r > x, (R_1 \ge ((\frac{P_2}{P_1})^{-\frac{1}{\alpha_1}} r^{\frac{\alpha_2}{\alpha_1}})] 2\pi \lambda_2 r e^{-\lambda_2 \pi r^2} \, \mathrm{d}r. \end{aligned} \tag{24}$$

Solving (24), $\mathbb{P}[R_2 > x, n = 2]$ can be derived as:

$$\mathbb{P}[R_2 > x, n = 2] = \begin{cases} \int_{x_1}^{x_2} \frac{R^2 - (\frac{P_2}{P_1})^{-\frac{2}{\alpha_1}} r^{\frac{2\alpha_2}{\alpha_1}}}{R^2 - z^2} 2\pi \lambda_2 r e^{-\lambda_2 \pi r^2} \, \mathrm{d}r \\ \quad + \int_x^{x_1} 2\pi \lambda_2 r e^{-\lambda_2 \pi r^2}, & x \le x_1, \\ \int_x^{x_2} \frac{R^2 - (\frac{P_2}{P_1})^{-\frac{2}{\alpha_1}} r^{\frac{2\alpha_2}{\alpha_1}}}{R^2 - z^2} 2\pi \lambda_2 r e^{-\lambda_2 \pi r^2} \, \mathrm{d}r, & x_2 \ge x > x_1, \\ 0, & x > x_2. \end{cases} \tag{25}$$

The CDF of X_2 is :

$$\begin{aligned} F_{X_2}(x) &= 1 - \mathbb{P}[X_2 > x] \\ &= 1 - \frac{1}{q_{U_2}} \mathbb{P}[R_2 > x, n = 2]. \end{aligned} \tag{26}$$

The PDF of X_2 is :

$$f_{X_2}(x) = \frac{dF_{X_2}}{dx} = \begin{cases} \frac{1}{q_{U_2}} (2\pi \lambda_2 x e^{-\lambda_2 \pi x^2}), & x \le x_1, \\ \frac{R^2 - (\frac{P_2}{P_1})^{-\frac{2}{\alpha_1}} x^{\frac{2\alpha_2}{\alpha_1}}}{R^2 - z^2} \frac{2\pi \lambda_2}{q_{U_2}} x e^{-\lambda_2 \pi x^2}, & x_2 \ge x > x_1, \\ 0, & x > x_2. \end{cases} \tag{27}$$

∎

Corollary 2. *The coverage probability of UEs in set U_2 is expressed in (28), and*

$$\mathcal{L}_{I_s} = \mathcal{L}_{I_s}(\mu T x^{\alpha_2}) = \exp\left(-\pi \lambda_2 x^2 (T P_2)^{2/\alpha_2} \operatorname{arccot}(T^{-2/\alpha_2}) \right) \times \exp\left(2\lambda_2 \int_{x_l}^{x_u} \frac{\arccos \frac{(D_{oo'}^2 + \rho^2 - z^2)}{(2 D_{oo'} \rho)}}{1 + \frac{\rho^{\alpha_2}}{P_2 s}} \rho \, \mathrm{d}\rho \right), \tag{29}$$

where $T = (2^{(U * N_{U_2} / W_{U_2})} - 1)/P_2$, W_{U_2} is the bandwidth allocated to set U_2, N_{U_2} is the average number of users in set U_2 and can be expressed as :$N_{U_2} = q_{U_2} \frac{\lambda_u}{\lambda_2}$. x_l can be written as $x_l = \max(D_{oo'} - z, x)$, $x_u = D_{oo'} + z$, and it is noted that $D_{oo'}$ has the constraints which can be expressed as $D_{oo'} \le (\frac{P_2}{P_1})^{-\frac{1}{\alpha_1}} x^{\frac{\alpha_2}{\alpha_1}}$, here we chose the upper bound $D_{oo'} = (\frac{P_2}{P_1})^{-\frac{1}{\alpha_1}} x^{\frac{\alpha_2}{\alpha_1}}$.

The proof of (29) can be referred to proof (60) based on Fig. 10 (c). Moreover, it is worth noting that because UEs in

$$G_{U_2}=\int_0^{x_1} e^{-\lambda_2\pi x^2}\frac{2\pi\lambda_2 x}{q_{U_2}}e^{-\mu T x^{\alpha_2}(I_m+\sigma^2)}\mathcal{L}_{I_s}\,\mathrm{d}x+\int_{x_1}^{x_2} e^{-\lambda_2\pi x^2}\frac{R^2-(\frac{P_2}{P_1})^{-\frac{2}{\alpha_1}}x^{\frac{2\alpha_2}{\alpha_1}}}{R^2-z^2}+\frac{2\pi\lambda_2 x}{q_{U_2}}e^{-\mu T x^{\alpha_2}(I_m+\sigma^2)}\mathcal{L}_{I_s}\,\mathrm{d}x. \tag{28}$$

set U_2 are likely to be close to small cells and far away from the macrocell, the approximation has a quite limited impact on the real results.

4) UEs in set U_3: In this part, an analysis of the coverage probability of UEs in set U_3 is provided. Just as shown in Fig. 2, set U_3 is the set of UEs in the CRE area. The set is expressed in (2).

The probability that a typical UE in set U_3 can be expressed as:

$$\begin{aligned}
&q_{U_3}\\
&=\mathbb{P}(P_1R_1^{-\alpha_1}\le P_2R_2^{-\alpha_2}B_2\cap P_1R_1^{-\alpha_1}\ge P_2R_2^{-\alpha_2})\\
&=\int_z^R\mathbb{P}((\frac{P_1}{P_2B_2})^{-\frac{1}{\alpha_2}}R_1^{\frac{\alpha_1}{\alpha_2}}\ge R_2\ge(\frac{P_1}{P_2})^{-\frac{1}{\alpha_2}}R_1^{\frac{\alpha_1}{\alpha_2}})f_{R_1}(r)\,\mathrm{d}r\\
&=\int_z^R(\exp(-\lambda_2\pi(\frac{P_1}{P_2})^{-\frac{1}{\alpha_2}}R_1^{\frac{\alpha_1}{\alpha_2}}))\frac{2r}{R^2-z^2}\,\mathrm{d}r\\
&-\int_z^R(\exp(-\lambda_2\pi(\frac{P_1}{P_2B_2})^{-\frac{1}{\alpha_2}}R_1^{\frac{\alpha_1}{\alpha_2}}))\frac{2r}{R^2-z^2}\,\mathrm{d}r.
\end{aligned}\tag{30}$$

The average number of users in set U_3 connect to the small cell is :$N_{U_3}=q_{U_3}\frac{\lambda_u}{\lambda_2}$.

Theorem 4. *The PDF $f_{X_3}(x)$ of the distance X_3 between a random UE in set U_3 with its associated small cell is:*

$$f_{X_3}(x)=\frac{dF_{X_3}}{dx}=\begin{cases}0, & x\le x_1\\ \frac{\rho_1^2-z^2}{q_{U_3}(R^2-z^2)}2\pi\lambda_2 x e^{-\lambda_2\pi x^2}, & x_1\le x<x_1^b,\\ \frac{\rho_1^2-\rho_2^2}{q_{U_3}(R^2-z^2)}2\pi\ \lambda_2 x e^{-\lambda_2\pi x^2}, & x_1^b<x\le x_2,\\ \frac{R^2-\rho_2^2}{q_{U_3}(R^2-z^2)}2\pi\ \lambda_2 x e^{-\lambda_2\pi x^2}, & x_2<x\le x_2^b,\end{cases}\tag{31}$$

where $x_1=\frac{z}{(\frac{P_2}{P_1})^{-0.25}}$, $x_1^b=\frac{z}{(\frac{P_2B_2}{P_1})^{-0.25}}$, $x_2=\frac{R}{(\frac{P_2}{P_1})^{-0.25}}$, $x_2^b=\frac{R}{(\frac{P_2B_2}{P_1})^{-0.25}}$. $\rho_1=(\frac{P_2}{P_1})^{-0.25}$. $\rho_2=(\frac{P_2B_2}{P_1})^{-0.25}$.

Proof: The event of $X_3>x$ is the event of $R_2>x$ conditioned on the UE's association to the third tier. The probability of $X_3>x$ can be expressed as:

$$\mathbb{P}[X_3>x]=\frac{\mathbb{P}[R_2>x,n=3]}{\mathbb{P}[n=3]}.\tag{32}$$

The joint probability of $R_2>x$ and n=3 is expressed in (33). Solving (33), $\mathbb{P}[R_2>x,n=3]$ can be written as (34).

The CDF of X_3 is :

$$\begin{aligned}F_{X_3}(x)&=1-\mathbb{P}[X_3>x]\\&=1-\frac{1}{q_{U_3}}\mathbb{P}[R_2>x,n=3].\end{aligned}\tag{35}$$

The PDF of X_3 is :

$$f_{X_3}(x)=\frac{dF_{X_3}}{dx}=\begin{cases}0, & x\le x_1\\ \frac{\rho_1^2-z^2}{q_{U_3}(R^2-z^2)}2\pi\lambda_2 x e^{-\lambda_2\pi x^2}, & x_1\le x<x_1^b,\\ \frac{\rho_1^2-\rho_2^2}{q_{U_3}(R^2-z^2)}2\pi\ \lambda_2 x e^{-\lambda_2\pi x^2}, & x_1^b\le x<x_2,\\ \frac{R^2-\rho_2^2}{q_{U_3}(R^2-z^2)}2\pi\ \lambda_2 x e^{-\lambda_2\pi x^2}, & x_2\le x<x_2^b.\end{cases}\tag{36}$$

■

Corollary 3. *The coverage probability of UEs in set U_3 can be expressed as:*

$$\begin{aligned}G_{U_3}=&\int_{x_1}^{x_1^b}e^{-\mu T x^{\alpha_2}\sigma^2-\lambda_2\pi x^2}\mathcal{L}_{I_s}(\mu T x^{\alpha_2})\frac{2\pi\lambda_2(\rho_1^2-z^2)}{q_{U_3}(R^2-z^2)}x\,\mathrm{d}x\\&+\int_{x_1^b}^{x_2}e^{-\mu T x^{\alpha_2}\sigma^2-\lambda_2\pi x^2}\mathcal{L}_{I_s}(\mu T x^{\alpha_2})\frac{2\pi\ \lambda_2(\rho_1^2-\rho_2^2)}{q_{U_3}(R^2-z^2)}x\,\mathrm{d}x\\&+\int_{x_2}^{x_2^b}e^{-\mu T x^{\alpha_2}\sigma^2-\lambda_2\pi x^2}\mathcal{L}_{I_s}(\mu T x^{\alpha_2})\frac{2\pi\ \lambda_2(R^2-\rho_2^2)}{q_{U_3}(R^2-z^2)}x\,\mathrm{d}x,\end{aligned}\tag{37}$$

where $x_1,x_2,x_1^b,x_2^b,\rho_1,\rho_2$ can be found in (31). $T=(2^{(U*N_{U_3}/W_{U_3})}-1)/P_2$, W_{U_3} is the bandwidth allocated to UEs in set U_3, N_{U_3} is the UEs in set U_3 and can be expressed as $N_{U_3}=q_{U_3}\frac{\lambda_u}{\lambda_2}$. Here, we provide an upper bound approximation of $\mathcal{L}_{I_s}$:

$$\begin{aligned}\mathcal{L}_{I_s}(\mu T x^{\alpha_2})=&\exp\left[2\lambda_2\int_{x_l}^{x_u}\frac{\arccos\frac{(D_{oo'}^2+\rho^2-z^2)}{(2D_{oo'}\rho)}}{1+\frac{\rho^{\alpha_s}}{P_2(s)}}\rho\,\mathrm{d}\rho\right]\\&\times\exp\left[-\lambda_2\pi x^2(TP_2)^{\frac{2}{\alpha_2}}\operatorname{arccot}(T^{-\frac{2}{\alpha_2}})\right],\end{aligned}\tag{38}$$

where $x_l=\max((\frac{P_2}{P_1})^{-\frac{1}{\alpha_1}}x^{\frac{\alpha_2}{\alpha_1}}-z,x)$, $x_u=(\frac{P_2}{P_1})^{-\frac{1}{\alpha_1}}x^{\frac{\alpha_2}{\alpha_1}}+z$, $D_{oo'}=(\frac{P_2}{P_1})^{-\frac{1}{\alpha_1}}x^{\frac{\alpha_2}{\alpha_1}}$.

Proof: See Appendix C ■

IV. Validation of Coverage Probability Analysis

In this section, we verify the developed analysis, in particular Theorem 1, Corollary 1, Corollary 2 and Corollary 3. The simulation parameters are listed in Table. I. The UE density here is assumed to be $0.0008/m^2$, and the small cell density is assumed to be $0.0005/m^2$. The small cell range expansion bias factor (B_2) is set to be 8dB. The coverage probability of UEs is validated by sweeping over a range of allocated bandwidth.

1) UEs in Set A: We suppose all UEs in set A will be offloaded to the macrocell. Fig. 3 explain the relationship between the bandwidth allocated and the coverage probability. We can easily see that with the increase of z, the coverage probability will decrease on a large scale. That is because

$$\begin{aligned}\mathbb{P}[R_2>x,n=3]&=\mathbb{P}[R_2>x,P_1R_1^{-\alpha_1}\le P_2R_2^{-\alpha_2}B_2\cap P_1R_1^{-\alpha_1}\ge P_2R_2^{-\alpha_2}]\\&=\int\mathbb{P}[r>x,P_1R_1^{-\alpha_1}\le P_2R_2^{-\alpha_2}B_2\cap P_1R_1^{-\alpha_1}\ge P_2R_2^{-\alpha_2}]2\pi\lambda_2re^{-\pi\lambda_2r^2}\,\mathrm{d}r\\&=\int\mathbb{P}[r>x,(\frac{P_2}{P_1})^{-\frac{1}{\alpha_1}}r^{\frac{\alpha_2}{\alpha_1}}\ge R_1\ge(\frac{P_2B_2}{P_1})^{-\frac{1}{\alpha_1}}r^{\frac{\alpha_2}{\alpha_1}}]2\pi\lambda_2re^{-\pi\lambda_2r^2}\,\mathrm{d}r.\end{aligned}\tag{33}$$

$$\mathbb{P}[R_2>x,n=3]=\begin{cases}\int_{x_1}^{x_1^b}\frac{\rho_1^2-z^2}{R^2-z^2}2\pi\lambda_2re^{-\lambda_2\pi r^2}\,\mathrm{d}r+\int_{x_1^b}^{x_2}\frac{\rho_1^2-\rho_2^2}{R^2-z^2}2\pi\ \lambda_2re^{-\lambda_2\pi r^2}\,\mathrm{d}r\\\quad+\int_{x_2}^{x_2^b}\frac{R^2-\rho_{1b}^2}{R^2-z^2}2\pi\ \lambda_2re^{-\lambda_2\pi r^2}\,\mathrm{d}r,x<x_1,\\\int_{x}^{x_1^b}\frac{\rho_1^2-z^2}{R^2-z^2}2\pi\lambda_2re^{-\lambda_2\pi r^2}\,\mathrm{d}r+\int_{x_1^b}^{x_2}\frac{\rho_1^2-\rho_2^2}{R^2-z^2}2\pi\ \lambda_2re^{-\lambda_2\pi r^2}\,\mathrm{d}r\\\quad+\int_{x_2}^{x_2^b}\frac{R^2-\rho_{1b}^2}{R^2-z^2}2\pi\ \lambda_2re^{-\lambda_2\pi r^2}\,\mathrm{d}r,x_1<x<x_1^b,\\\int_{x_1^b}^{x_2}\frac{\rho_1^2-\rho_2^2}{R^2-z^2}2\pi\ \lambda_2re^{-\lambda_2\pi r^2}\,\mathrm{d}r+\int_{x_2}^{x_2^b}\frac{R^2-\rho_2^2}{R^2-z^2}2\pi\ \lambda_2re^{-\lambda_2\pi r^2}\,\mathrm{d}r,x_1^b<x<x_2,\\\int_{x_2}^{x_2^b}\frac{R^2-\rho_2^2}{R^2-z^2}2\pi\ \lambda_2re^{-\lambda_2\pi r^2}\,\mathrm{d}r,x_2<x<x_2^b,\\0,\quad x>x_2^b.\end{cases}\tag{34}$$

TABLE I
SYSTEM PARAMETERS IN THE NUMERICAL COMPUTATION

Macro/small cell /UE distribution	hexagon/PPP /uniform distribution
Density of UEs [m^2]	0.0002×[1,2,...,10]
Bandwidth allocation [MHz]	20
Power consumption of macrocells (P_1) [W]	40
Power consumption of small cells (P_2) [W]	1
Number of antennas (N_{AT})	1
Noise power(σ^2) [dbm]	-104
Macro/small cell pathloss exponent (α_1/α_2)	4
P_{0M}, P_{0S} [W]	130, 6.8
Δ_{pm}, Δ_{ps}	4.7 ,4.0
P_{mM}, P_{mS} [W]	20.0, 0.5
$P_s(s)$ [W]	0
Date rate requirement (U) [Mbps]	0.64
Coverage probability Threshold (η)	0.8
CRE bias factor for small cells (B_2) [db]	[0,4,8,12]
Macrocell size (apothem of hexagon) [m]	500

with the increase of z, more UEs will be offloaded to the macrocell from the sleeping small cells. In that case, more bandwidth is needed from the macrocell to guarantee the coverage probability of its UEs.

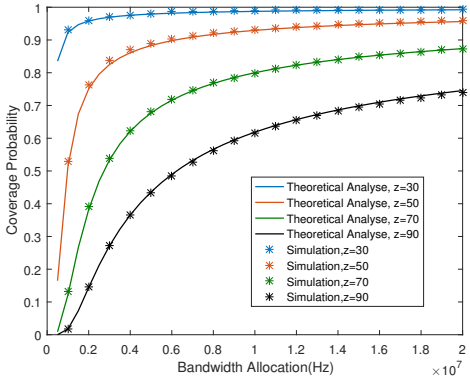

Fig. 3. Coverage probability obtained from simulation and Theorem 1(G_A) for UEs in set A

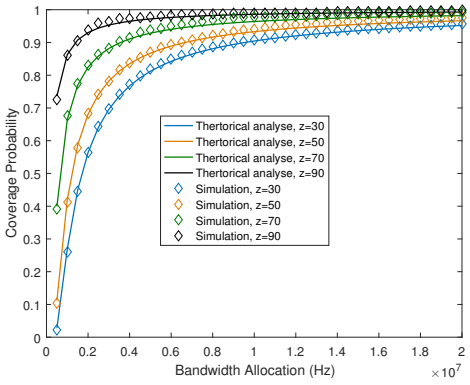

Fig. 4. Coverage probability obtained from simulation and Corollary 1(G_{U_1}) for UEs in set U_1

2) UEs in Set U_1: The relationship between the allocated bandwidth and the coverage probability of the UEs in set U_1 is shown in Fig. 4. It can be seen that as z increases, the coverage probability of UEs increases steadily, the major reason of which is the number of UEs in set U_1 decreases with the increasing of z. Recalling that the set U_1 is the set of UEs connected to macrocell outside the dashed circle, with the increase of z, the number of UEs in set U_1 declines. We demonstrate this as follows:

$$\begin{aligned}N_{U_1}&=q_{U_1}\pi(R^2-z^2)\\&=\pi(R^2-z^2)\lambda_u\int_z^R e^{-\lambda_2(\frac{P_1}{P_2B})^{-\frac{2}{\alpha_2}}r^{\frac{2\alpha_1}{\alpha_2}}}\frac{2r}{R^2-z^2}\,\mathrm{d}r,\end{aligned}\tag{39}$$

where N_{U_1} is the number of UEs in set U_1, and q_{U_1} is the association probability which can be found in (12). With numerical calculation, we can find that N_{U_1} goes down rapidly with the increase of z.

3) UEs in Set U_2: The relationship between the allocated bandwidth and the coverage probability of UEs in set U_2 is shown in Fig. 5. In order to show the difference of coverage

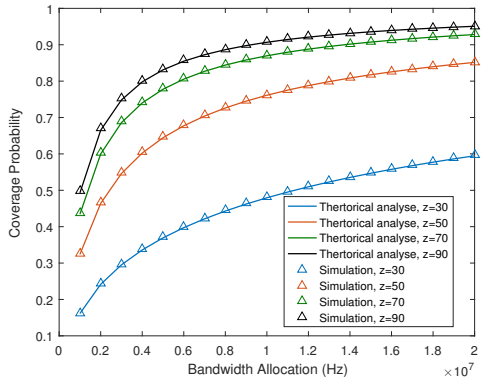

Fig. 5. Coverage probability obtained from simulation and Corollary 2(G_{U_2}) for UEs in set U_2

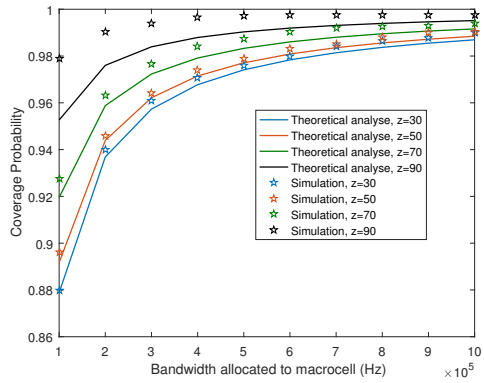

Fig. 6. Coverage probability obtained from simulation and Corollary 3(G_{U_3}) for UEs in set U_3

probability for each z significantly, we chose the maximum I_m here, $I_m = P_1 z^{-\alpha_1}$. From Fig. 5, we can see that the coverage probability of UEs rises with the increase of z, the reason of which is the interference from the macrocell to UEs in set U_2 decreases with the increase of z, hence, the coverage probability will increase correspondingly.

4) UEs in Set U_3: The relationship between the allocated bandwidth and the coverage probability of UEs in set U_3 is illustrated in Fig. 6. It is noted that in this part, the inter cell interference from small cells cannot be calculated accurately, hence, we provide an approximation of the upper bound of the interference. We can also see that the coverage probability of UEs rises with the increase of z, this is because the number of UEs in set U_3 goes down with the increase of z. We demonstrate this as follows:

$$N_{U_3} = q_{U_3} \frac{\lambda_u}{\lambda_2}, \tag{40}$$

where N_{U_3} is the number of UEs in set U_3, q_{U_3} is the UEs' association probability to set U_3, which can be found in (30). With numerical integration, we can find that N_{U_3} decreases when the increase of z.

V. Energy Saving Problems Analysis and Solutions

Based on the derived coverage constraints in (10), (19), (28) and (37) in the section III, we analyse the minimum power consumption with given UE density. The network power consumption can be written as shown in (41), where P_{0M}, Δ_{pm}, P_{mM}, Δ_{ps} and P_{sS} can be found in Table. I. Our problem is to minimize the whole network power consumption with given UE density($\theta(t)$), while guaranteeing the QoS of all UEs. The problem can be formulated as below:

$$\begin{aligned}
\text{OPT:}\ & \min P(\lambda_2, z, B_2) && (42)\\
& G_A(z, W_A, B_2, \lambda_2) > \eta && (43)\\
& G_{U_1}(z, W_{U_1}, B_2, \lambda_2) > \eta && (44)\\
& G_{U_2}(z, W_{U_2}, \lambda_2) > \eta && (45)\\
& G_{U_3}(z, W_{U_3}, B_2, \lambda_2) > \eta && (46)\\
& W_A + W_{U_1} + W_{U_3} \leq W_t && (47)\\
& W_{U_2} + W_{U_3} \leq W_t && (48)\\
& B_2 \in [0, 4, 8, 12] && (49)
\end{aligned}$$

However, the problem is hard to solve as there is no closed-form expressions for W_A, W_{U_1}, W_{U_2}, W_{U_3} in (10),(19),(28),(37) respectively. Hence, we solve the problem step by step.

Firstly, for each $B_2 \in [0, 4, 8, 12]$, we calculate the lower bound and upper bound of z, which can be written as z_{min} and z_{max}. Here, we assume $z_{min} = 0$, and z_{max} can be calculated according to (43), (44) and (47) with the minimum $\lambda_2(min)$. It is noted that $\lambda_2(min)$ can be derived easily according to (45) and (49).

Then, we use genetic algorithm (GA) [34] to calculate the minimum network power consumption $P^*(B_2)$ for each B_2.

Finally, we compare $P^*(B_2)$ with each B_2 and found the minimum one.

Below is the summarized optimization steps:

1) Let $z_{min} = 0$ and derive z_{max} according to (43), (44), (46) and (47) .
2) Derive $\lambda_2(min)$ from (45) and (49) for each z.
3) With given $\lambda_2(min)$, use genetic algorithm to calculate the minimum network power consumption $P^*(B_2(i))$ in terms of z with each B_2. Constraints need to be satisfied.
4) Find the minimum value of $\{P^*(B_2(i))\}$

We utilize the bi-objective optimization algorithm of MATLAB Optimization toolbox to implement our algorithm. The pseudocode of GA is shown in Algorithm 1.

Fig. 7 and Fig. 8 illustrate the network energy consumption with different z and different bias factor. It is noted that in order to guarantee the QoS of UEs in the situation of $B_2 = 1$, orthogonal bandwidth is used by the macrocell and small cells to avoid the inter-cell interference. Comparing the two figures, it is easy to see that the network has a higher power consumption with more UEs. Also, both two figures demonstrate that the network consumes lower power with larger small cell bias factor (B_2). Furthermore, we can also see that when $B_2 = 0$, the network power consumption decreases slightly with the increase of z, however, with CRE technique used, especially with large B_2, the network power consumption drops rapidly, that is because the small cell density outside the dashed circle is diluted in a large scale with CRE technique applied.

$$P = (P_{0M} + \Delta_{pm} P_{mM} \frac{W_A + W_{U1}}{W_t} + (P_{0S} + \Delta_{ps} P_{sS} \frac{W_{U2} + W_{U3}}{W_t}))\lambda_2 \pi (R^2 - z^2), \quad (41)$$

Algorithm 1 Genetic algorithm solving for the optimal values of f(z)

Input: target function data, GA parameters
Output: minimum power consumption

: t=0
: // P(t): population of current generation
// FitnessFunction $\forall z \in P(t)$, $f(z) = (P_{0M} + \Delta_{pm} \cdot P_{mM} \cdot \frac{W_A + W_{U1}}{W_t} + (P_{0S} + \Delta_{ps} \cdot P_{sS} \cdot \frac{W_{U2} + W_{U3}}{W_t})\lambda_2 \pi (R^2 - z^2))$
//Constraints
: Initialize P(t)
: while (not termination condition) do
: Fitness = FitnessFunction(P(t)), P(t)'= Selection(P(t)), Genetic Operations(P(t)')
: Select P(t+1) from P(t) and P(t)'
: t=t+1
: end while

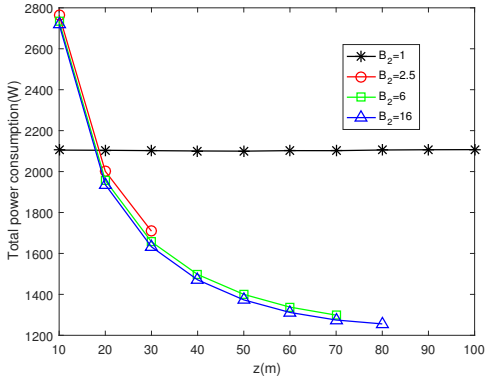

Fig. 7. Network power consumption with switching off radius with $\theta = 0.0016$

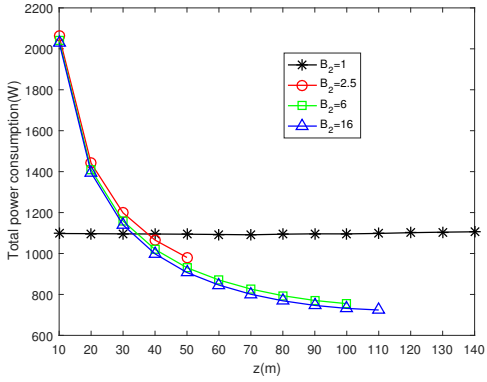

Fig. 8. Network power consumption with switching off radius with $\theta = 0.0008$

Fig. 9 represents the relationship between the total network power consumption with different UE density for the three approaches. Both random and conventional methods are used

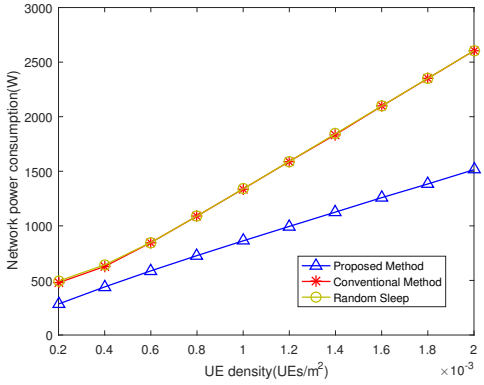

Fig. 9. Network power consumption with different UE density

in traditional HeNets and the orthogonal bandwidth is used by the two layers for both approaches to avoid the inter-cell interference.

For the conventional method from [27], we suppose that we only switch off small cells of which distance to the macrocell smaller than z. Similar to (10), (19) and (28), the coverage probability of UEs can be written as (50), where $\mathcal{L}_{I_s}$ is expressed in (29). The network power consumption can be written similar to (41) without W_{U_3}. The optimization procedure is similar to what we mentioned in Section V.

For the random method, we randomly turn off small cells to the lowest level that can guarantee the QoS of UEs.

When comparing the conventional and random methods, it can be seen that the performance of the conventional method is only a little better than that of the random one, the reason of which is that offloading UEs from sleeping small cells to the macrocell will result in the power consumption increase of the macrocell. Moreover, as the remaining small cells outside the dashed circle are all left to be active, this will also lead to a high network power consumption.

We can also see that our proposed sleeping scheme achieves a far better performance than that of conventional and random ones by combining small cell zooming and small cell sleeping techniques together. With CRE and eICIC techniques used here, the small cells density outside the dashed circle can be significantly diluted, especially with a higher UE density. It can be seen from the figure that when the UE density reaches $2 * 10^{(-3)}/\mathrm{m}^2$, the network power consumption of our proposed method is about 1500W, which is only 60% compared with that of the conventional approach.

VI. Conclusion

In this paper, a strategic small cell sleeping mechanism according to the dynamic traffic is proposed to minimize the HetNet power consumption. Our proposed approach uses range expanded small cells to cover part of the sleeping small

$$\begin{cases} G_A(\text{con}) = \int_0^z e^{-\mu T r^{\alpha_1}\sigma^2}\frac{2r}{z^2}\,\mathrm{d}r. \\ G_{U_1}(\text{con}) = \int_z^R e^{-\lambda_2\pi(\frac{P_1}{P_2})^{-\frac{2}{\alpha_2}}x^{\frac{2\alpha_1}{\alpha_2}}}e^{-\mu T x^{\alpha_1}\sigma^2}\frac{2x}{q_{U_1}(R^2-z^2)}\,\mathrm{d}x. \\ G_{U_2}(\text{con}) = \int_0^{x_1} e^{-\lambda_2\pi x^2}\frac{2\pi\lambda_2 x}{q_{U_2}}e^{-\mu T x^{\alpha_2}(\sigma^2)}\mathcal{L}_{I_s}\,\mathrm{d}x + \int_{x_1}^{x_2} e^{-\lambda_2\pi x^2}\frac{R^2-(\frac{P_2}{P_1})^{-\frac{2}{\alpha_1}}x^{\frac{2\alpha_2}{\alpha_1}}}{R^2-z^2}\frac{2\pi\lambda_2 x}{q_{U_2}}e^{-\mu T x^{\alpha_2}\sigma^2}\mathcal{L}_{I_s}\,\mathrm{d}x, \end{cases} \tag{50}$$

cells which are far from the macrocell and uses the macrocell to serve the UEs from the sleeping cells close to it. Using stochastic geometry model, we provide the numerical analysis of the coverage probability and power saving in a HetNet. Numerical results confirm the effectiveness of the scheme. Compared with the random and conventional approaches, the proposed repulsive scheme achieves a much better performance, especially when the UE density is high.

For future work, the LOS/NLOS probability transitions need to be taken into account. In addition, a more realistic network model, for example, Poisson cluster point process based network model should be considered. Moreover, a more detailed UE association scheme should be designed.

VII. Appendix

A. Proof of Theorem 1

The coverage probability of UEs in area A can be written as:

$$\begin{aligned} G_A &= \mathbb{E}\left\{\mathbb{P}\left[\frac{W_A}{N_A}\log_2(1+\gamma_A) > U\right]\right\} \\ &= \mathbb{E}_r\left\{\mathbb{P}\left[\frac{W_A}{N_A}\log_2(1+\frac{P_1 h r^{-\alpha_m}}{I_s+\sigma^2}) > U\right]\right\} \\ &= \int_0^z \mathbb{P}\left[\frac{W_A}{N_A}\log_2(1+\frac{P_1 h r^{-\alpha_m}}{I_s+\sigma^2}) > U\right] f_R(r)\,\mathrm{d}r \\ &= \int_0^z \mathbb{P}\left[h > \frac{(2^{\frac{UN_A}{W_A}}-1)(I_s+\sigma^2)r^{\alpha_1}}{P_1}\right]\frac{2r}{z^2}\,\mathrm{d}r \\ &= \int_0^z e^{-\mu T r^{\alpha_1}\sigma^2}\mathcal{L}_{I_s}(\mu T r^{\alpha_1})\frac{2r}{z^2}\,\mathrm{d}r. \end{aligned} \tag{51}$$

Replacing $\mu T r^{\alpha_1}$ with s, $\mathcal{L}_{I_s}(s)$ can be derived as:

$$\begin{aligned} \mathcal{L}_{I_s}(s) &= \mathbb{E}\left(\exp\left(-s\textstyle\sum_{x\in\phi\cap b^c(o',z)} P_2 h_{x,o}||x||^{-\alpha_2}\right)\right) \\ &= \mathbb{E}_\phi\left(\textstyle\prod_{x\in\phi\cap b^c(o',z)}\mathbb{E}_{h_{x,o}}[\exp(-sP_2 h_{x,o})||x||^{-\alpha_2})]\right) \\ &= \mathbb{E}_\phi\left(\textstyle\prod_{x\in\phi\cap b^c(o',z)}(1+sP_2||x||^{-\alpha_2})^{-1}\right) \\ &= \exp\left(\int_{b^c(o',z)}\frac{\lambda_2}{1+\frac{||x||^{\alpha_2}}{(sP_2)}}\,\mathrm{d}x - \int_{\mathbb{R}^2}\frac{\lambda_2}{1+\frac{||x||^{\alpha_2}}{(sP_2)}}\,\mathrm{d}x\right). \end{aligned} \tag{52}$$

When $\alpha = \alpha_1 = \alpha_2 = 4$, using $s = \mu T r^{\alpha_1}$, we have

$$\int_{\mathbb{R}^2}\frac{1}{1+||x||^{\alpha}/(sP_2)}\,\mathrm{d}x = \frac{\left[\pi r (TP_2)^{\frac{1}{\alpha}}\right]^2}{2}. \tag{53}$$

In Fig. 10a, o' is the location of macrocell, and o is the location of UE, the distance between o and o' is r. For $\int_{b^c(o',z)}\frac{1}{1+||x||^{\alpha_2}/(sP_2)}\,\mathrm{d}x$, $b^c(o',z)$ is the disk with centre o' and radius z, x is the coordinate of the small cell. Convert the integration $\int_{b^c(o',z)}\frac{1}{1+||x||^{\alpha_2}/(sP_2)}\,\mathrm{d}x$ from Cartesian to polar coordinates with origin o, then:

$$\begin{aligned} &\int_{b^c(o',z)}\frac{1}{1+||x||^{\alpha_2}/(sP_2)}\mathrm{d}x \\ &\quad= \int_{b^c(o',z)}\frac{1}{1+\rho^{\alpha_2}/(sP_2)}\rho d\rho d\theta \\ &\quad= \int_0^{z-r}\int_{-\pi}^{\pi}\frac{1}{1+\rho^{\alpha_2}/(sP_2)}\rho d\rho d\theta \\ &\qquad+ \int_{z-r}^{z+r}\int_{-\theta_l}^{\theta_l}\frac{1}{1+\rho^{\alpha_2}/(sP_2)}\rho d\rho d\theta \\ &\quad= \int_0^{z-r}\frac{2\pi}{1+\frac{\rho^{\alpha_2}}{P_2 s}}\rho\,\mathrm{d}\rho + \int_{z-r}^{z+r}\frac{2\theta_l}{1+\frac{\rho^{\alpha_2}}{P_2 s}}\rho\,\mathrm{d}\rho, \end{aligned} \tag{54}$$

where $\theta_l = \arccos(\frac{r^2+\rho^2-z^2}{2r\rho})$.

Then, $\mathcal{L}_{I_s}(s)$ in Theorem 1 can be expressed as (55).

B. Proof of $\mathcal{L}_{I_s}(\mu T x^{\alpha_1})$ in Corollary 1

Replacing $\mu T x^{\alpha_1}$ with s, similar to (52), $\mathcal{L}_{I_s}(s)$ can be expressed as:

$$\begin{aligned} \mathcal{L}_{I_s}(s) &= \mathbb{E}\left(\exp\left(-s\textstyle\sum_{x'\in\phi\cap b^c(o',z)} P_2 h_{x,o}||x'||^{-\alpha_2}\right)\right) \\ &= \exp\left(\int_{\mathbb{R}^2\setminus sl}\frac{-\lambda_2}{1+\frac{||x'||^{\alpha_2}}{(sP_2)}}\,\mathrm{d}x' - \int_{b^c(o',z)}\frac{-\lambda_2}{1+\frac{||x'||^{\alpha_2}}{(sP_2)}}\,\mathrm{d}x'\right), \end{aligned} \tag{56}$$

where sl is the set of the small cells whose distance to the UE is smaller than $(\frac{P_1}{P_2 B_2})^{-\frac{1}{\alpha_2}}x$, which is derived according to (15).

When $\alpha = \alpha_1 = \alpha_2 = 4$, plugging in $s = \mu T x^{\alpha_1}$, (56) can be written in the form of (57).

In Fig. 10b, o' is the position of macrocell, o is the position of UE, because the user is served by the macrocell, the distance between o and o' is x. For $\int_{b^c(o',z)}\frac{1}{1+||x'||^{\alpha_2}/(sP_2)}\,\mathrm{d}x'$, $b^c(o',z)$ is the disk with centre o' and radius z, x' is the coordinate of the small cell. Convert the integration $\int_{b^c(o',z)}\frac{1}{1+||x'||^{\alpha_2}/(sP_2)}\,\mathrm{d}x'$ from Cartesian to polar coordinates with origin o, then:

$$\begin{aligned} &\int_{b^c(o',z)}\frac{1}{1+||x'||^{\alpha_2}/(sP_2)}\,\mathrm{d}x' \\ &\quad= \int_{b^c(o',z)}\frac{1}{1+\rho^{\alpha_2}/(sP_2)}\rho\mathrm{d}\rho\mathrm{d}\theta \\ &\quad= \int_g^{x+z}\int_{-\theta_l}^{\theta_l}\frac{1}{1+\rho^{\alpha_2}/(sP_2)}\rho\mathrm{d}\rho\mathrm{d}\theta \\ &\quad= \int_g^{x+z}\frac{2\theta_l}{1+\rho^{\alpha_2}/(sP_2)}\rho\mathrm{d}\rho, \end{aligned} \tag{58}$$

where $\theta_l = \arccos(\frac{x^2+\rho^2-z^2}{2x\rho})$, and $g = \max((\frac{P_1}{P_2 B_2})^{-1/\alpha_2}\cdot x, x-z)$.

Then, $\mathcal{L}_{I_s}$ in Corollary 1 can be written in (59), and $m = (\frac{P_1}{P_2 B_2})^{-0.5}$.

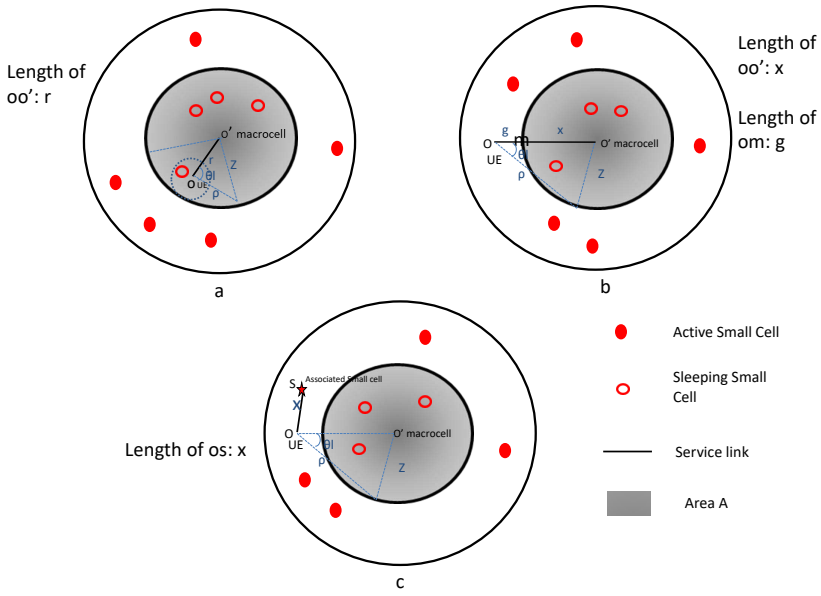

Fig. 10. Illustration of interference Laplace transform proof

$$\mathcal{L}_{I_s}(s)=\exp\left(-\frac{\left[\pi r(TP_2)^{\frac{1}{\alpha}}\right]^2}{2}\right)\exp\left(2\lambda_2\int_{r-z}^{r+z}\frac{\arccos(\frac{r^2+\rho^2-z^2}{2r\rho})}{1+\frac{\rho^{\alpha_2}}{P_2 s}}\rho\,\mathrm{d}\rho+2\lambda_2\int_0^{r-z}\frac{\pi}{1+\frac{\rho^{\alpha_2}}{P_2 s}}\rho\,\mathrm{d}\rho\right). \tag{55}$$

$$\exp\left(-\lambda_2\left(\int_{\mathbb{R}^2\setminus sl}\frac{1}{1+||x'||^{\alpha_2}/(sP_2)}\,\mathrm{d}x'\right)\right)=\exp\left(-2\pi\lambda_2\int_{(\frac{P_1}{P_2B_2})^{-\frac{1}{\alpha_2}}x}^{+\infty}\frac{T}{T+(v/x)^{\alpha}}v\mathrm{d}v\right)$$
$$=\exp\left(-\lambda_2\pi x^2(T\ P_2)^{2/\alpha}\mathrm{arccot}((\frac{P_1}{P_2B_2})^{-2/\alpha_2}\cdot T^{-2/\alpha})\right). \tag{57}$$

$$\mathcal{L}_{I_s}(s)=\exp\left(-\lambda_2\pi x^2(TP_2)^{2/\alpha}\,\mathrm{arccot}(mT^{-2/\alpha})\right)\exp\left(2\lambda_2\int_g^{r+z}\frac{\theta_l}{1+\frac{\rho^{\alpha_2}}{P_2\cdot s}}\rho\mathrm{d}\rho\right). \tag{59}$$

C. Proof of $\mathcal{L}_{I_s}(\mu T x^{\alpha_2})$ in Corollary 3

Replacing $\mu T x^{\alpha_2}$ with s, similar to (52), $\mathcal{L}_{I_s}(s)$ can be expressed as:

$$\mathcal{L}_{I_s}(s)=\mathbb{E}\left(\exp\left(-s\sum_{x\in\phi\cap b^c(o',z)\setminus o}P_2h_{x,o}||x||^{-\alpha_2}\right)\right]$$
$$=\exp\left(\left(\int_{\mathbb{R}^2\setminus o}\frac{-\lambda_2}{\frac{1+||x||^{\alpha_2}}{(sP_2)}}\,\mathrm{d}x-\int_{b^c(o',z)}\frac{-\lambda_2}{\frac{1+||x||^{\alpha_2}}{(sP_2)}}\,\mathrm{d}x\right)\right), \tag{60}$$

when $\alpha_2=4$, plugging in $s=\mu T x^{\alpha_2}$ gives

$$\exp\left(-\lambda_2\left(\int_{\mathbb{R}^2\setminus o}\frac{1}{1+||x||^{\alpha_2}/(sP_2)}\,\mathrm{d}x\right)\right)$$
$$=\exp\left(-2\pi\lambda_2\int_x^{+\infty}(\frac{T}{T+(v/x)^{\alpha}}v\mathrm{d}v\right) \tag{61}$$
$$=\exp\left(-\lambda_2\pi x^2(T\cdot P_2)^{2/\alpha_2}\,\mathrm{arccot}(T^{-2/\alpha_2})\right).$$

In Fig. 10(c), o' is the location of macrocell and o is location of UE. The distance between the associated small cell s and UE in o is x, and I assume that the distance between o and o' is $D_{oo'}$. It's worth noting that based on (33), $D_{oo'}$ must satisfy the condition that $((\frac{P_2}{P_1})^{-\frac{1}{\alpha_1}}x^{\frac{\alpha_2}{\alpha_1}}\geq D_{oo'}\geq(\frac{P_2B}{P_1})^{-\frac{1}{\alpha_1}}x^{\frac{\alpha_2}{\alpha_1}})$. For $\int_{b^c(o',z)}\frac{1}{1+||x||^{\alpha_2}/(sP_2)}\,\mathrm{d}x$, $b^c(o',z)$ is the disk with centre o' and radius z, x is the coordinate of the small cell. Convert the integration $\int_{b^c(o',z)}\frac{1}{1+||x||^{\alpha_2}/(sP_2)}\,\mathrm{d}x$ from Cartesian to polar coordinates with origin o, then:

$$\begin{aligned}&\int_{b^c(o',z)}\frac{1}{1+||x||^{\alpha_2}/(sP_2)}\,\mathrm{d}x\\&=\int_{b^c(o',z)}\frac{1}{1+\rho^{\alpha_2}/(sP_2)}\rho\mathrm{d}\rho\mathrm{d}\theta\\&=\int_{x_l}^{x_u}\int_{-\theta_l}^{\theta_l}\frac{1}{1+\rho^{\alpha_2}/(sP_2)}\rho\mathrm{d}\rho\mathrm{d}\theta\\&=\int_{x_l}^{x_u}\frac{2\theta_l}{1+\rho^{\alpha_2}/(sP_2)}\rho\mathrm{d}\rho,\end{aligned} \tag{62}$$

where $\theta_l=\arccos\frac{(D_{oo'}^2+\rho^2-z^2)}{(2D_{oo'}\rho)}$, x_u can be expressed as $x_u=D_{oo'}+z$, and x_l can be written as $x_l=\max(D_{oo'}-z,x)$, also, it can be seen that the upper bound of $\mathcal{L}_{I_s}(s)$ is $D_{oo'}=$

$(\frac{P_2}{P_1})^{-\frac{1}{\alpha_1}} x^{\frac{\alpha_2}{\alpha_1}}$, and lower bound is $(\frac{P_2 B_2}{P_1})^{-\frac{1}{\alpha_1}} x^{\frac{\alpha_2}{\alpha_1}}$. I choose upper bound here.

Then, $\mathcal{L}_{I_s}(s)$ in Corollary 3 is expressed in (63),

$$\mathcal{L}_{I_s}(s) = \exp\left(-\lambda_2 \pi x^2 (T \cdot P_2)^{2/\alpha_2} \operatorname{arccot}(T^{-2/\alpha_2})\right) \times \exp\left(2\lambda_2 \int_{x_l}^{x_u} \frac{\arccos \frac{(D_{oo'}^2 + \rho^2 - z^2)}{(2 D_{oo'} \rho)}}{1 + \frac{\rho^{\alpha_2}}{s P_2}} \rho \, \mathrm{d}\rho\right), \tag{63}$$

where $x_l = \max((\frac{P_2}{P_1})^{-\frac{1}{\alpha_1}} x^{\frac{\alpha_2}{\alpha_1}} - z, x), x_u = (\frac{P_2}{P_1})^{-\frac{1}{\alpha_1}} x^{\frac{\alpha_2}{\alpha_1}} + z, D_{oo'} = (\frac{P_2}{P_1})^{-\frac{1}{\alpha_1}} x^{\frac{\alpha_2}{\alpha_1}}$.

ACKNOWLEDGMENT

The authors would like to thank Jiliang Zhang whose constructive and detailed comments helped us a lot to improve the quality of the paper.

REFERENCES

[1] I. Hwang, B. Song, and S. S. Soliman, "A holistic view on hyper-dense heterogeneous and small cell networks," *IEEE Communications Magazine*, vol. 51, no. 6, pp. 20–27, 2013.

[2] G. Fettweis and E. Zimmermann, "Ict energy consumption-trends and challenges," in *Proceedings of the 11th international symposium on wireless personal multimedia communications*, vol. 2, no. 4. (Lapland, 2008, p. 6.

[3] A. Fehske, G. Fettweis, J. Malmodin, and G. Biczok, "The global footprint of mobile communications: The ecological and economic perspective," *IEEE Communications Magazine*, vol. 49, no. 8, 2011.

[4] T. Langedem, "Reducing the carbon footprint of ict devices, platforms and networks," *GreenTouch, Amsterdam, The Netherlands*, Nov. 2012.

[5] L. Belkhir and A. Elmeligi, "Assessing ict global emissions footprint: Trends to 2040 & recommendations," *Journal of Cleaner Production*, vol. 177, pp. 448–463, 2018.

[6] A. S. Andrae and T. Edler, "On global electricity usage of communication technology: trends to 2030," *Challenges*, vol. 6, no. 1, pp. 117–157, 2015.

[7] I. Ashraf, F. Boccardi, and L. Ho, "Sleep mode techniques for small cell deployments," *Communications Magazine, IEEE*, vol. 49, no. 8, pp. 72–79, 2011.

[8] Z. Niu, "Tango: Traffic-aware network planning and green operation," *IEEE Wireless Communications*, vol. 18, no. 5, 2011.

[9] M. A. Marsan, L. Chiaraviglio, D. Ciullo, and M. Meo, "Optimal energy savings in cellular access networks," in *Communications Workshops, 2009. ICC Workshops 2009. IEEE International Conference on*. IEEE, 2009, pp. 1–5.

[10] E. Oh, K. Son, and B. Krishnamachari, "Dynamic base station switching-on/off strategies for green cellular networks," *IEEE transactions on wireless communications*, vol. 12, no. 5, pp. 2126–2136, 2013.

[11] W. Guo and T. O'Farrell, "Dynamic cell expansion with self-organizing cooperation," *IEEE Journal on Selected Areas in Communications*, vol. 31, no. 5, pp. 851–860, 2013.

[12] F. Han, Z. Safar, and K. R. Liu, "Energy-efficient base-station cooperative operation with guaranteed qos," *Communications, IEEE Transactions on*, vol. 61, no. 8, pp. 3505–3517, 2013.

[13] A. Bousia, A. Antonopoulos, L. Alonso, and C. Verikoukis, "" green" distance-aware base station sleeping algorithm in lte-advanced," in *Communications (ICC), 2012 IEEE International Conference on*. IEEE, 2012, pp. 1347–1351.

[14] W. Guo and T. O'Farrell, "Green cellular network: Deployment solutions, sensitivity and tradeoffs," in *Wireless Advanced (WiAd), 2011*. IEEE, 2011, pp. 42–47.

[15] D. Tsilimantos, J.-M. Gorce, and E. Altman, "Stochastic analysis of energy savings with sleep mode in ofdma wireless networks," in *INFOCOM, 2013 Proceedings IEEE*. IEEE, 2013, pp. 1097–1105.

[16] Y. Li, H. Celebi, M. Daneshmand, C. Wang, and W. Zhao, "Energy-efficient femtocell networks: Challenges and opportunities," *IEEE Wireless Communications*, vol. 20, no. 6, pp. 99–105, 2013.

[17] S. Wang and W. Guo, "Energy and cost implications of a traffic aware and quality-of-service constrained sleep mode mechanism," *IET Communications*, vol. 7, no. 18, pp. 2092–2101, 2013.

[18] E. Mugume and D. K. So, "Spectral and energy efficiency analysis of dense small cell networks," in *Vehicular Technology Conference (VTC Spring), 2015 IEEE 81st*. IEEE, 2015, pp. 1–5.

[19] L. Saker, S.-E. Elayoubi, R. Combes, and T. Chahed, "Optimal control of wake up mechanisms of femtocells in heterogeneous networks," *IEEE Journal on Selected Areas in Communications*, vol. 30, no. 3, pp. 664–672, 2012.

[20] S.-r. Cho and W. Choi, "Energy-efficient repulsive cell activation for heterogeneous cellular networks," *IEEE Journal on Selected Areas in Communications*, vol. 31, no. 5, pp. 870–882, 2013.

[21] Y. S. Soh, T. Q. Quek, M. Kountouris, and H. Shin, "Energy efficient heterogeneous cellular networks," *IEEE Journal on Selected Areas in Communications*, vol. 31, no. 5, pp. 840–850, 2013.

[22] C. Liu, B. Natarajan, and H. Xia, "Small cell base station sleep strategies for energy efficiency," *IEEE Transactions on Vehicular Technology*, vol. 65, no. 3, pp. 1652–1661, 2016.

[23] D. Cao, S. Zhou, and Z. Niu, "Optimal combination of base station densities for energy-efficient two-tier heterogeneous cellular networks," *IEEE Transactions on Wireless Communications*, vol. 12, no. 9, pp. 4350–4362, 2013.

[24] J. Peng, H. Tang, P. Hong, and K. Xue, "Stochastic geometry analysis of energy efficiency in heterogeneous network with sleep control," *IEEE Wireless Communications Letters*, vol. 2, no. 6, pp. 615–618, 2013.

[25] J. Kim, W. S. Jeon, and D. G. Jeong, "Effect of base station-sleeping ratio on energy efficiency in densely deployed femtocell networks," *IEEE Communications Letters*, vol. 19, no. 4, pp. 641–644, 2015.

[26] A. Prasad, A. Maeder, and C. Ng, "Energy efficient small cell activation mechanism for heterogeneous networks," in *Globecom Workshops (GC Wkshps), 2013 IEEE*. IEEE, 2013, pp. 754–759.

[27] S. Zhang, J. Gong, S. Zhou, and Z. Niu, "How many small cells can be turned off via vertical offloading under a separation architecture?" *IEEE Transactions on Wireless Communications*, vol. 14, no. 10, pp. 5440–5453, 2015.

[28] P. Dini, M. Miozzo, N. Bui, and N. Baldo, "A model to analyze the energy savings of base station sleep mode in lte hetnets," in *Green computing and communications (GreenCom), 2013 IEEE and internet of things (iThings/CPSCom), IEEE international conference on and IEEE cyber, physical and social computing*. IEEE, 2013, pp. 1375–1380.

[29] R. Tao, J. Zhang, and X. Chu, "An energy saving small cell sleeping mechanism with cell expansion in heterogeneous networks," in *Vehicular Technology Conference (VTC Spring), 2016 IEEE 83rd*. IEEE, 2016, pp. 1–5.

[30] D. Lopez-Perez, S. Güvenç, G. De la Roche, M. Kountouris, T. Q. Quek, and J. Zhang, "Enhanced intercell interference coordination challenges in heterogeneous networks," *Wireless Communications, IEEE*, vol. 18, no. 3, pp. 22–30, 2011.

[31] H. Zhou, Y. Ji, X. Wang, and S. Yamada, "eicic configuration algorithm with service scalability in heterogeneous cellular networks," *IEEE/ACM Transactions on Networking (TON)*, vol. 25, no. 1, pp. 520–535, 2017.

[32] H. S. Dhillon, R. K. Ganti, F. Baccelli, and J. G. Andrews, "Modeling and analysis of k-tier downlink heterogeneous cellular networks," *IEEE Journal on Selected Areas in Communications*, vol. 30, no. 3, pp. 550–560, 2012.

[33] H.-S. Jo, Y. J. Sang, P. Xia, and J. G. Andrews, "Heterogeneous cellular networks with flexible cell association: A comprehensive downlink sinr analysis," *IEEE Transactions on Wireless Communications*, vol. 11, no. 10, pp. 3484–3495, 2012.

[34] K. Deb, A. Pratap, S. Agarwal, and T. Meyarivan, "A fast and elitist multiobjective genetic algorithm: Nsga-ii," *IEEE transactions on evolutionary computation*, vol. 6, no. 2, pp. 182–197, 2002.

Ran Tao received the B.S. degree in electronic and communication engineering from the Univeristy of Liverpool, UK. He is currently pursuing the Ph.D. degree with the Communication Group, Department of Electronic and Electrical Engineering, The University of Sheffield, U.K. His research interests include green communication, heterogeneous networks, wireless backhaul, and stochastic geometry.

Wuling Liu received the B.E. degree from Xian Jiaotong University, China, in 2009, and the M.E. degree from Southeast University, China, in 2012. He is currently pursuing the Ph.D. degree in electrical engineering with The University of Sheffield, U.K. His research interests include information theory and communications theory.

Xiaoli Chu received the Ph.D. degree from The Hong Kong University of Science and Technology, in 2005. She is a Reader with The University of Sheffield. From 2005 to 2012, she was with Kings College London. She has authored over 80 peer-reviewed journal and conference papers. She is a leading editor/author of the book Heterogeneous Cellular Networks (Cambridge University Press: 2013). She was the Co-Chair of Wireless Communications Symposium for the IEEE ICC 2015, and the Guest Editor for the IEEE TRANSACTIONS ON VEHICULAR TECHNOLOGY and ACM/Springer Journal of Mobile Networks and Applications.

Jie Zhang is currently a Full Professor and has been the Chair in Wireless Systems with the EEE Department, The University of Sheffield, Sheffield, U.K., since 2011. He was with Imperial College London, Oxford University, and the University of Bedfordshire. He and his students have pioneered research in femto/small cell and HetNets and published some of the earliest and most widely cited publications in these topics (three of top ten most cited). He co-founded RANPLAN Wireless Network Design Ltd. that produces a suite of world leading in-building DAS, indoor-outdoor small cell/HetNet network design, and optimization tools iBuildNet-Professional, Tablet, DAS, and Manager. Since 2005, he has been awarded over 20 research projects by the EPSRC, the EC FP6/FP7/H2020, and the industry, including some of earliest projects on femtocell/HetNets.